NUCLEAR STRUCTURE STUDIES ON EXOTIC NUCLEI BY DIRECT REACTIONS IN INVERSE KINEMATICS

P. Egelhof

Gesellschaft für Schwerionenforschung GSI, D 6100 Darmstadt, Germany

I. Introduction

The new heavy-ion accelerator facilities [1,2] at GSI, which came into operation in 1990, provide new opportunities for a variety of nuclear studies. With respect to exotic nuclei the unique combination of the heavy-ion synchrotron SIS, the fragment separator FRS and the experimental storage ring ESR (see fig. 1) is of interest. The SIS delivers primary heavy-ion beams presently with intensities up to a few times 10^9 sec^{-1}. In combination with the FRS secondary exotic beams with high energies (100 MeV/u up to 1-2 GeV/u) are produced and isotopically selected. These beams can be either used directly for experiments, or injected and stored into the ESR and cooled to highest phase space densities [1] ($\Delta p/p \leq 10^{-6}$, $\varepsilon \leq 0.1\pi$ mm mrad) and optionally decelerated. These possibilities open a variety of nuclear structure studies in the region away from stability. In the present contribution we want to focus on the investigation of direct reactions with such exotic beams.

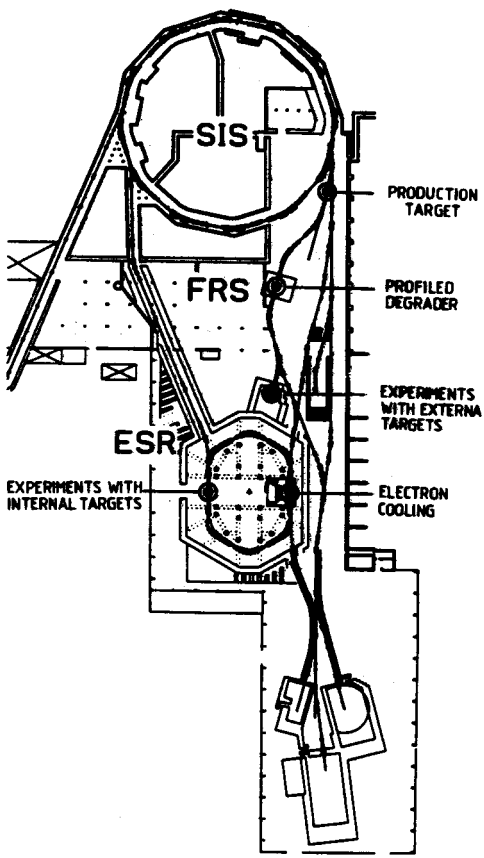

Fig. 1: Layout of the new heavy-ion accelerator facility at GSI. It consists of the heavy-ion synchrotron SIS, the fragment separator FRS and the storage cooler ring ESR. Direct reaction studies with exotic beams in inverse kinematics are alternatively performed using external targets directly behind the fragment separator or using internal targets in the storage ring.

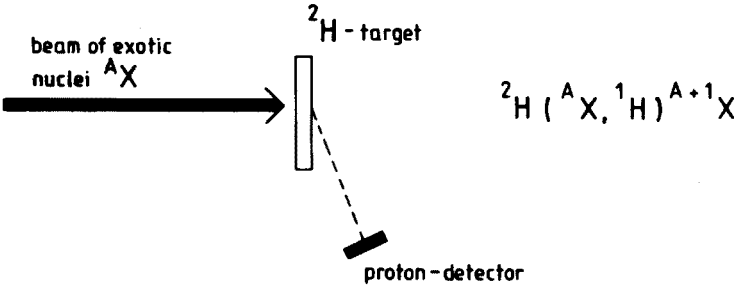

Fig. 2: The method of inverse kinematics is sketched for the example of a (d,p)-reaction on the nucleus ^{A}X.

A classical method to obtain spectroscopic information is the investigation of light ion induced direct reactions, i.e. one- and few-nucleon transfer reactions, inelastic and elastic scattering. This method was up to recently limited to stable or very long lived nuclei, which allow to produce stable targets. The availability of good quality radioactive beams allows now to study such reactions on exotic nuclei using the method of inverse kinematics, which is sketched in fig. 2 for the example of a (d,p)-reaction.

In the next section the physics motivation and the physics program are described, followed by a discussion of the experimental concept. In the last section the status of a few selected first generation experiments will be discussed.

II. Motivation and Physics Program

In principle a large variety of light ion induced reactions may be investigated for various reasons. One- and few-nucleon transfer reactions, such as (d,p), (p,d), (d,t), (d,^{3}He), (^{3}He,t), (^{3}He,α), etc., are used to populate single particle (hole)-states or two particle (two hole)-states, whereas inelastic (p,p'), (α,α') etc. scattering leads to the population of collective states. In addition (p,p), (d,d), (α,α), etc., elastic scattering may be used to investigate nuclear potentials. In the following a few selected examples will be discussed in detail.

II.1. Transfer Reactions

The localization of single particle states, including the determination of their orbital angular momentum and their spectroscopic strength, allows a test of the nuclear shell model in the region away from stability. Here the question of new regions of shell closures may be investigated. A parametrization of single particle proton energies throughout the valley of stability was recently established by Mairle et al. [3]. It will be of course interesting to test the predictions of such a parametrization in the region away from stability.

Of particular interest are few nucleon transfer reactions on nuclei at or in close vicinity to doubly closed shells, such as ^{56}Ni and ^{132}Sn [4]. Here matrix elements of the residual two-body interaction as derived from the particle-particle- and particle-hole - multiplett states in adjacent even - A nuclei may be investigated. As compared to such investigations in the region of semi-magic nuclei, the doubly magic ^{56}Ni (Z = 28, N = 28) and ^{132}Sn (Z = 50, N = 82) -cores should simplify the analysis and interpretation of the data considerably and many ambiguities may be removed. For ^{132}Sn information on the two-body residual interaction for a large number of new combinations of shell model orbits is expected, which could nearly double the available information on two-body matrix elements in doubly magic nuclei. At present only ^{48}Ca and ^{208}Pb in the region of stability are comparable cases [5]. While measurements around the exotic ^{132}Sn might be of most interest, less spectacular radioactive beams, such as ^{55}Co, ^{57}Ni, ^{57}Cu in the vicinity of ^{56}Ni and beams in the vicinity of ^{48}Ca (^{47}Ca, ^{47}K, ^{49}Ca, ^{49}Sc) and ^{208}Pb (^{207}Tl, ^{209}Pb) may give important additional information.

The investigation of neutron pickup reactions, such as (d,p)-reactions, is of considerable interest for astrophysical questions, namely for the understanding of the synthesis of stable isotopes in stellar burning processes. Here the determination of neutron resonances (E_n, l_n, spectroscopic factors) for a couple of neutron rich nuclei may be the basis for improved calculations of neutron capture cross sections [6], especially for alternative astrophysical environments, for example those with different neutron densities. Of special interest is the region of the observed isotopic anomalies [7]. Recent theoretical investigations (n-capture [8] and NSE-models [9]) localize the region of interest to nuclei near ^{46}K, ^{50}Ca, ^{51}Ti, ^{56}Cr, ^{61}Fe, ^{66}Ni, etc. [10]. In addition, spectroscopy on radioactive nuclei in the ^{20}Na-region may yield new insight in the r p - process [11].

II.2. Elastic Scattering

The investigation of elastic scattering on exotic nuclei enables to deduce information on nuclear potentials and on nuclear matter densities. Of particular interest is (p,p)-scattering on light neutron rich nuclei at high energies (around 1 GeV/u), as was proposed by G.D. Alkhazov et al. [12]. From such data the nuclear matter-distributions may be investigated, as was successfully done in the past for a large variety of stable nuclei [13]. The techniques of inverse kinematics with radioactive beams enables such investigations for nuclei far off stability. As examples of special interest the neutron rich light helium- and lithium-isotopes (especially a comparison of ^{9}Li and ^{11}Li to investigate the question of the neutron halo [14,15]) may be considered. For such investigations the high incident energies (around 1 GeV/u) which are available now at GSI are of considerable advantage as compared to elastic scattering at lower incident enegies [16], because the mechanism of proton-nucleus scattering at higher energies is simple, and thus the theoretical interpretation of the data is more straight forward and unambiguous.

Another topic of interest is the investigation of the isospin dependence of nucleus-nucleus potentials which may be derived from a comparison of elastic scattering of two isobaric nuclei as projectiles, for example ^{18}O (^{14}C, ^{14}C) ^{18}O and ^{18}O (^{14}O, ^{14}O) ^{18}O, as proposed by A. Ogloblin et al. [17].

II.3. Inelastic Scattering

A variety of interesting questions is connected with the investigation of inelastic scattering on exotic nuclei [4]. Inelastic scattering to low lying collective states should not only locate these states, but yield information on their collective strength, deformation parameters, and transition densities. High spin states will dominate the spectra for processes with larger momentum transfer. Therefore we may be able to localize some of the stretched-configuration high spin states. Of particular interest is also the localization and transition strength of the 1^+-magnetic dipole states, which are core excitations of spin-orbit partners, i.e. particle-hole excitations with maximum radial overlap between the particle and the hole. The strength of these unnatural parity states can be directly connected to the Gamow-Teller strength in nuclear beta decay. For more details the reader may be referred to reports on studies on stable nuclei performed at Indiana and Los Alamos [18].

III. Experimental Concept

In order to study reactions to resolved final states in the heavy nucleus it is advantageous to detect the light recoil nucleus. Quantities of interest for direct reactions are:

i) the energies of the light particles in the exit channel from which the nuclear level schemes may be deduced.

ii) the structure of the angular distributions from which the spins (at least the l-values) may be deduced. For transfer reactions there exists a rather close relation between the position of the first diffraction maximum and the transfered orbital angular momentum l.

iii) the absolute cross sections from which spectroscopic factors, collective strength and optical potentials may be deduced.

Generally for direct reaction studies the forward angular region $0° \lesssim \vartheta_{cm} \lesssim 60°$ is of most interest. The energy resolution needed is of the order of the nuclear level spacings, typically of the order of $\Delta E = 50 - 100$ keV. Typical cross sections are of the order of 1-100 mb/sr. These conditions lead to severe constraints for the quality of the exotic beams and for the experimental setup, which are different for different kinds of reactions, as will be displayed in the following sections. Before focussing in detail on the kinematical conditions of the experiments to be performed in inverse kinematics the procedure how to produce and handle the secondary beams will be briefly discussed in the following section.

III.1. Production and Handling of Secondary Beams

The method to produce beams of radioactive nuclei in the fragment separator FRS is displayed schematically in figure 3 (see also references 2 and 19). Incident stable heavy ion beams with energies between 100 MeV/u and 2000 MeV/u are delivered from the heavy ion synchrotron SIS and transported to the production target of the FRS. For the isotopic separation of the projectile fragments with relativistic energies they are analyzed with respect to their magnetic rigidity and their energy loss.

The FRS consists of four independent stages, each including a 30°-dipole magnet and a set of quadrupole magnets for focussing. In the achromatic operation mode (shown in figure 3) a shaped energy degrader is installed after the second stage. The isotopic separation is obtained in 2 steps (see lower part of figure 3). Due to the reaction kinematics the fragments are separated with respect to their A/Z-ratio after the second stage of the FRS. The energy loss of the ions penetrating the degrader provides a different A- and Z-dependent isotopic selection at the final focal plane. By matching the velocity dispersions with the appropriately shaped energy degrader, this separation can be made velocity independent. Finally, beams of individual isotopes, well separated in space, are obtained, providing the following features:

- due to the production method (projectile fragmentation) the energies of the secondary beams are above about $E \geq 100$ MeV/u.
- the beam emittance is about $\varepsilon \leq 20\pi$ mm mrad.
- the longitudinal momentum spread is of the order of $\Delta p/p \leq \pm 1\%$.

As discussed in more detail below, these beams from the FRS may be used directly for selected experiments in inverse kinematics with external targets (see also figure 1), or they may be injected into the experimental storage ring ESR to improve the beam qualities and to tune their energies.

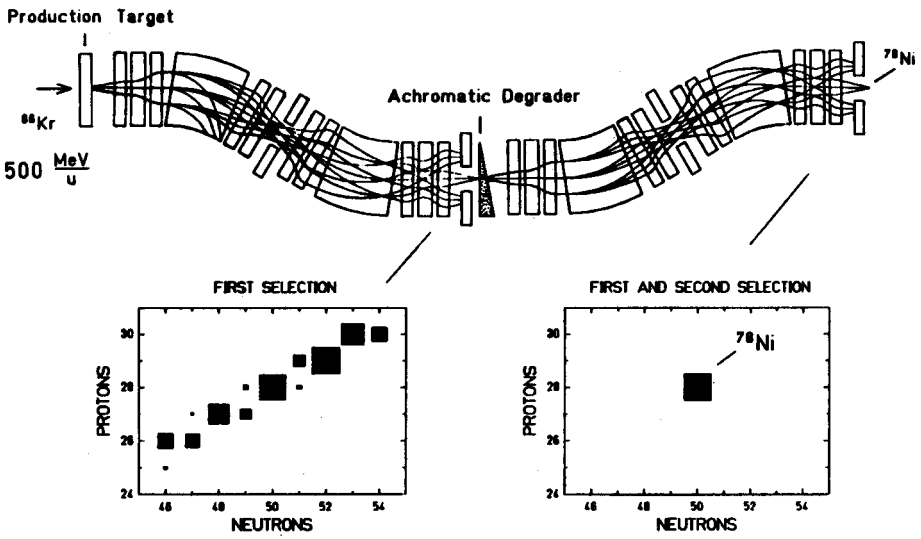

Fig. 3: The operation principle of the fragment separator FRS at GSI is displayed schematically for the example of the exotic fragment ^{78}Ni, produced via fragmentation of ^{86}Kr at an incident energy of E = 500 MeV/u (figure taken from reference 19). The areas for the different isotopes displayed in the lower part of the figure are proportional to the corresponding calculated transmission rates.

The layout of the ESR [1] is displayed in figure 4. For our purposes its most important components are the electron cooler, which provides beam cooling to highest phase space densities, rf-cavities which allow to tune the beam energy, and the internal gas-jet target [1,20] (H_2, He, O_2, etc.), which may be used as interaction target for the experiments in inverse kinematics. In recent experiments [1,21] it was demonstrated that electron cooling provides excellent beam qualities, even for heaviest ions, and that the simultaneous storage of different ion charge states is possible. In addition the successful transfer of secondary beams from the FRS to the ESR, as well as the stacking, storage and cooling at such secondary beams was reported [22].

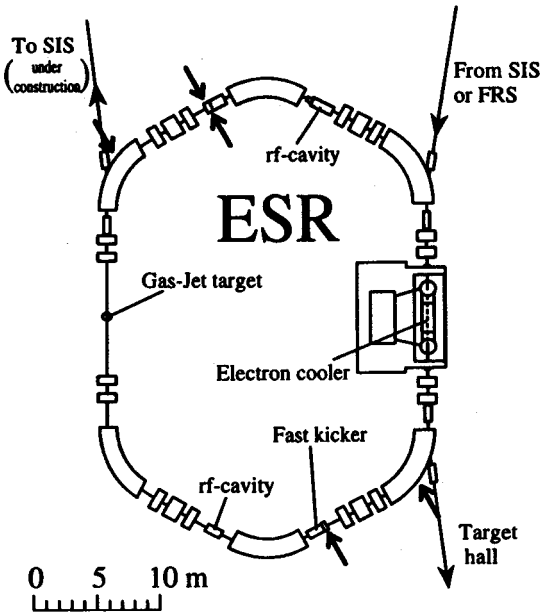

Fig. 4: Layout of the experimental storage ring ESR (for details see text).

In summary the ESR provides

- excellent qualities of the secondary beams: $\varepsilon \leq 0.1\ \pi$ mm mrad, $\frac{\Delta p}{p} \leq 10^{-6}$,
- the tuning of the beam energy down to about E≤5 MeV/u,
- the use of the internal gas-jet target which allows for low background (pure H_2), and high luminosities due to many beam-target interactions (revolution frequency $f = 10^5$-10^6 sec^{-1}, see below).

Single nucleon transfer reactions are best performed at energies of about 10-15 MeV/u, dependent on the Q-values in individual cases. The arguments for the choice of this energy range are momentum matching for the transfer to states of fairly low angular momentum, i.e. the corresponding single particle configurations. Under these conditions the structure in the angular distributions is characteristic of the transfered angular momentum and the extraction of the spectroscopic strength in terms of a DWBA-analysis is straightforward. At higher incident energies the analysis of the data is no longer as unambiguous due to the higher order processes enhanced by the momentum mismatch between the transfered nucleon in projectile and target, leading to a loss in cross section and l-selectivity [4,23]. In contrast, incident energies between 100 MeV/u and 1 GeV/u are desirable for elastic and inelastic scattering in order to optimize excitation probabilities, and to allow for an unambiguous analysis of elastic scattering data, as mentioned already above.

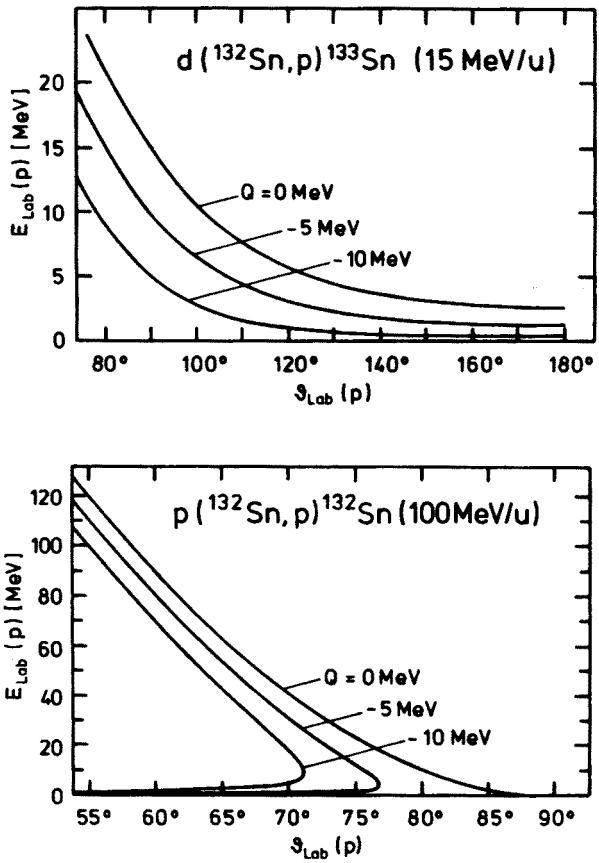

Fig. 5: Kinematics (proton energy $E_{Lab}(p)$ versus proton angle $\vartheta_{Lab}(p)$) for the reaction d(^{132}Sn,p)^{133}Sn at an incident energy of 15 MeV/u (upper part) and for the reaction p(^{132}Sn, p)^{132}Sn at 100 MeV/u (lower part).

Figure 5 displays, as examples, the kinematical conditions for (d,p)- reactions (upper part) and (p,p)- and (p,p')- elastic and inelastic scattering (lower part) on ^{132}Sn. For the case of the (d,p)-reactions the emitted protons of interest cover an angular range of $75° < \vartheta_{lab} < 180°$, even for rather large negative Q-values. The proton energies are of the order of E_p < 20 MeV and the average $dE / d\theta_{lab} < 0.4$ *MeV/deg* , thus standard detector systems with an angular resolution of $\Delta\theta \lesssim 0.25°$ will be sufficient for the most cases.

For (p,p)- and (p,p')- reactions the situation is quite different. The backscattered protons of interest cover the angular range $60° < \theta_{lab} < 90°$ with proton energies up to $E_p \approx 80$ MeV. The variation of the proton energy with the laboratory angle reaches values of up to $dE / d\theta_{lab} = 6$ *MeV/deg*, thus requiring high angular resolution of about $\Delta\theta \approx 0.02°$ in order to obtain a reasonable energy resolution.

III.3. Required Features of Secondary Beams and the Experimental Setups

The basic properties of the secondary beams and the experimental setups are determined by the optimization of the incident energy, the energy resolution and the counting rates. Dependent on the special conditions of each experiment measurements may be performed at GSI either at the experimental area directly behind the FRS, using conventional external targets, or with stored radioactive beams circulating in the storage ring using internal ESR-targets (see section III.1 and fig. 1).

For transfer reactions the radioactive beams produced in the FRS have to be injected into the ESR in order to decelerate them to energies around 10-15 MeV/u. This is because at GSI-conditions the exotic beams are produced [2] at considerably higher energies, typically above $E \geq 100$ *MeV/u* . For the investigation of elastic and inelastic scattering no deceleration will be necessary, but in many cases storing and cooling of the beam to highest phase space densities [1,21] ($\varepsilon \lesssim 0.1\pi$ mm mrad, $\Delta p/p \leq 10^{-6}$) in the ESR will be essential to obtain sufficient energy resolution.

For special conditions, such as short nuclear lifetimes ($\tau_{nucl} \leq 1$ sec), which do not allow for injection and cooling in the storage ring, and large nuclear level spacing, which does not require highest energy resolution to resolve neighbouring energy levels, experiments with beams directly from the FRS at external target stations without using the ESR are foreseen. Under these conditions the quality of the exotic beams from the FRS [2], ($\varepsilon \leq 20\ \pi$ mm mrad, $\Delta p/p \leq \pm 1\%$), will allow to receive a sufficient energy resolution.

As external targets $(CH_2)_n$-foils with a thickness up to d ≤ 1 mg/cm² (limited by the amount of multiple scattering in the target) are used. For special conditions active targets, such as H_2- or He-filled time projection ionization chambers allow much higher luminosities (see section IV). As internal target in the ESR a gas-jet target [1,20] with a density up to 10^{14} atoms/cm² and a size of about 3-5 mm in diameter may be used. Here the relatively small target thickness is compensated for by the repetition rate of the beam and the possibility to stack the beam in order to reach highest luminosities (see next section). To obtain high angular resolution internal fibre targets containing hydrogen (d < 10 μm in diameter) may be used, which provide a well localized interaction zone [24]. For the future also an internal polarized hydrogen target is foreseen [24,25], which allows to study the spin de-

pendent part of direct reactions. This allows, for example, the determination not only of l, but of j in transfer reactions.

The intensities of secondary exotic beams from the FRS are mainly limited by the intensities of the incident primary beams available from SIS, and the cross sections for fragmentation. In table 1 estimates for a few examples are displayed. The numbers given were calculated assuming a FRS production target of 4 g/cm^2 ^{9}Be and a primary beam intensity of 5x10^8 sec^{-1} at an incident energy of 350 MeV/u. It should be pointed out that the assumed primary beam intensities are realistic for GSI-conditions at the present time [1], at least for ions with $A \leq 100$, and may be even improved in the near future. The fragmentation cross sections were taken from calculations performed by K. Sümmerer et al. [26]. In addition the transmission through the FRS was taken into account with typical values around 25 %. The estimates displayed in table 1 were verified in a recent experiment [27] with ^{56}Ni, where a secondary beam intensity of 2-3x10^4 sec^{-1} ^{56}Ni-ions was obtained.

For a typical experiment at an external target, for example (p,p')-inelastic scattering on ^{56}Ni, as discussed in detail in section IV, the expected event rate for inelastically scattered protons was estimated assuming typical values around 20 mb/sr for the differential cross section [28], a 1 mg/cm^2 thick $(CH_2)_n$ -target and a total useful solid angle covered by the detectors of $\Omega = 150$ msr. The resulting expected event rate of 46/h shows, that the present conditions allow first generation experiments to be performed for several cases of interest (see section II). On the other hand it becomes clear from table 1 that some of the most interesting cases in the region far off stability, such as nuclei in the vicinity of the doubly magic ^{132}Sn, will only be possible after a considerable improvement of the experimental conditions. Essential for such experiments will be:

- an improvement of the primary beam intensities (ion source, high current injector, transfer efficiency UNILAC→SIS): => increase in event rates: factor 3-30.
- use of large area detector systems, covering the whole useful solid angle: => factor 5-10.
- use of the internal ESR gas target in combination with continuous beam accumulation and stacking (see also next section): => factor 3-100.

Isotope	Projectile	Production Cross Section $\sigma[\mu b]$	Intensity [sec^{-1}]
^{56}Ni	^{58}Ni	1400	$5 \cdot 10^4$
^{56}Cr	^{64}Ni	2200	$8 \cdot 10^4$
^{61}Fe	^{64}Ni	4300	$1.5 \cdot 10^5$
^{132}Sn	^{136}Xe	0.5	$2 \cdot 10^1$

Table 1: Expected production cross sections and intensities of secondary beams provided by the fragment separator. The numbers given are calculated assuming a primary beam intensity of 5x10^8 sec^{-1} at an incident energy of 350 MeV/u and a production target of 4 g/cm^2 ^{9}Be (for further details see text).

III.4. Comparison of the Conditions for the Use of External and Internal ESR-Targets

The accumulation and storage of exotic beams in the experimental storage ring ESR and the use of internal interaction targets may be of considerable advantage, not only for the quality of the exotic beams due to beam cooling, but also for the luminosities. A survey of the performance of the ESR for physics with exotic beams is given in ref.[29]. In the present context a comparison between the conditions for the use of an external target setup and for an internal storage ring target for direct reactions in inverse kinematics will be discussed. Here external targets may be either used with the direct beams from the FRS (as already discussed in the previous sections), or with cooled and (or) decelerated beams extracted from the ESR.

For our comparison we will deal with the following assumptions:

- The thickness of an external $(CH_2)_n$-target, used as a hydrogen target, is limited to about $d \leq 1 mg/cm^2$ in order to keep the amount of multiple scattering of the beam and the outgoing light particles at a tolerable level. This assumption holds for most of the experiments to be considered.
- The density of the internal ESR gas-jet target is assumed to be 10^{14} atoms/cm^2, which corresponds to the design value [20].
- The intensity of the secondary beam from the FRS is assumed to be $5 \cdot 10^4$/sec (see table 1).
- The exotic beam from the FRS will be continuously accumulated, cooled and stacked in the storage ring.
- As a total useful nuclear cross section (differential cross section times detector solid angle) we assume $\sigma_{nucl} = 3$ mb, which is reasonable for both inelastic scattering (see previous section), as well as for transfer reactions, where the differential cross sections are smaller, but the useful solid angle that can be covered is generally considerably larger.

Under these conditions we expect for an external target, with only one passage of the beam through the target, an event rate of 46/h. For the conditions of the internal ESR target we take advantage of the fact that many beam - target interactions with a typical repetition rate of 10^5-10^6 sec^{-1} are possible. The relevant number to be considered is the ratio of the nuclear cross section and the cross section which leads to a loss of the beam out of the ESR. We assume charge exchange processes in the internal target to be the dominant loss process (besides nuclear decay of the exotic nuclei, see below). The fully stripped beam injected into the ESR will undergo electron capture and consequently be lost. The electron capture cross sections are strongly dependent on the nuclear charge and the energy of the beam. For the present estimates we use scaling laws from Schlachter et al. [30] (for the lower energies), and from Stöhlker et al. [31,32] (see also ref. [29]). For the example of a 10 MeV/u $^{56}Ni^{28+}$-beam we obtain an electron capture cross section of $\sigma_{atom} = 5.4 \times 10^{-22} cm^2$ leading to a lifetime of the beam in the storage ring of $\tau_{atom} = 47$ sec, and a ratio between nuclear and electron capture cross section $\sigma_{nucl}/\sigma_{atom} = 5.6 \times 10^{-6}$. Taking into account the production rate of the exotic beam we expect an average event rate of about 1000/h, which represents for this case an advantage of the internal over the external target of a factor 22. In fig. 6 the ratio of event rates obtained with an internal target R_{Int} and with an external target R_{Ext} is plotted versus the nuclear charge Z_P of the beam for incident energies of 10 MeV/u and 100 MeV/u. Due to the Z_P - and E-dependence of the charge exchange cross

section we obtain the displayed dependence of R_{Int}/R_{Ext} . For the case of the lower beam energy (solid line in fig. 6) a "break even" point $R_{Int}/R_{Ext} = 1$ is reached for heavier beams, where the lifetime of the beam in the storage ring is only of the order of a few seconds. It should be pointed out that the situation may be still improved by using the possibility of multiple charge state operation of the ESR [1,21]. On the other hand, we have to take into account in addition the transfer efficiency for the beam between the FRS and the ESR, which depends on the quality of the exotic beam in each individual case.

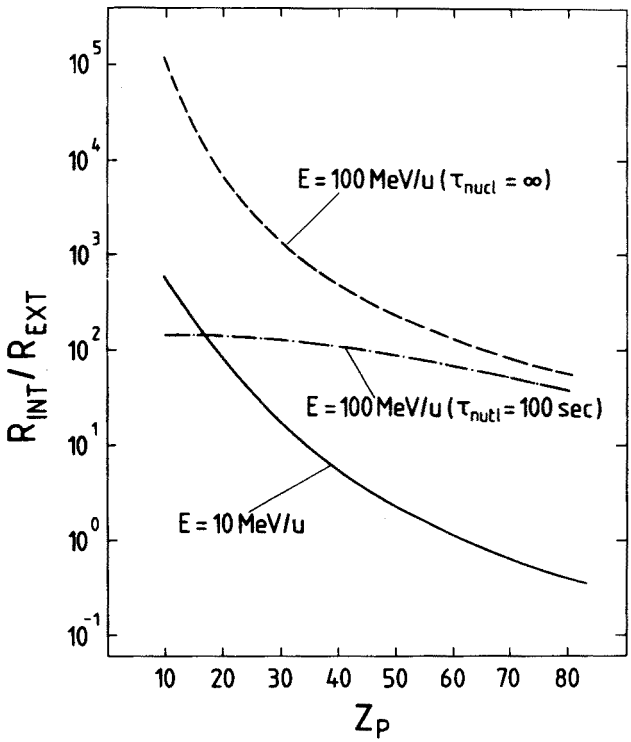

Fig. 6: The ratio of event rates R_{Int}/R_{Ext} expected for a direct reaction in inverse kinematics, investigated using an internal hydrogen gas jet target (R_{Int}) and an external $(CH_2)_n$-target (R_{Ext}), is plotted versus the nuclear charge Z_p of the projectile. The situation is displayed for beam energies of 10 MeV/u (solid line) and of 100 MeV/u, in the latter case for a nuclear lifetime of $\tau_{nucl} = \infty$ (dashed line) and of $\tau_{nucl} = 100$ sec (dashed-dotted line). The experimental conditions which were assumed for the present calculations are listed in the text.

For the case of the higher beam energy the gain for the internal target may be orders of magnitude higher (dashed line) due to the longer lifetimes of the beams in the storage ring (for example $\tau_{atom} = 1200$ sec for $Z_P = 28$). Of course in

this case we have to take into account the nuclear lifetime of exotic beams which might contribute considerably to the loss processes of the beams in the ring. As compared to the dashed line (for infinite nuclear lifetime of the exotic beams), the dashed-dotted line, where a nuclear lifetime of $\tau_{nucl} = 100$ sec was assumed, is more realistic for the case of the higher energies. Here an improvement of about 2 orders of magnitude, almost independent of the nuclear charge of the projectile, is expected. This demonstrates the advantage of using internal targets for many situations and justifies the effort for performing experiments in the technically challenging UHV-environment of heavy-ion storage rings.

IV. Status of First Experiments

In this section a few selected first generation experiments will be discussed. The status of experimental developments for these experiments, as well as first results will be displayed.

IV.1. Investigation of (p,p')-Inelastic Scattering on ^{56}Ni

As a first prototype experiment with an external target (p,p')-inelastic scattering on the doubly magic nucleus ^{56}Ni to the first excitated state at 2.70 MeV has been investigated at an incident energy of E = 100 MeV/u. This experiment is intended to yield a more accurate value for the poorly known [33,34] matrix element for the transition connecting the 0^+-ground state to the first excited 2^+-state, and therefore to allow a more sensitive test of shell model calculations for that nucleus. In addition this experiment provides a good test case for addressing the problems associated with doing inverse reactions with radioactive beams. The first diffraction maximum in the angular distribution of the inelastic cross section for the excitation to the 2.70 MeV 2^+-state in ^{56}Ni (expected at $\Theta_{CM} = 12° - 18°$) is localized between $\vartheta_{lab} = 78.5°$ and $\vartheta_{lab} = 80.9°$ in the laboratory system for the inverse kinematics. Due to the large level spacing in ^{56}Ni the inelastically scattered protons to the 2^+-state are energetically well separated from the elastic protons (see fig. 7).

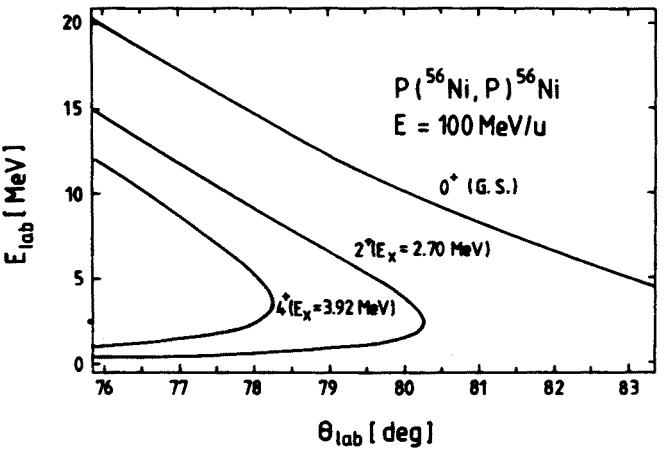

Fig. 7: Kinematics (proton energy E_{Lab} versus proton angle θ_{lab}) for p(^{56}Ni,p)^{56}Ni -elastic scattering (G.S.) and inelastic scattering to excited states at E_x = 2.70 MeV and E_x = 3.92 MeV at an incident energy of E = 100 MeV/u.

This allows to resolve inelastic scattering from elastic, even with a large angular acceptance of the detector system ($\Delta\vartheta_{lab} = 2°$), and when using the direct beam from the FRS with an energy spread of about $\Delta E = 2.5\%$ without beam cooling in the ESR.

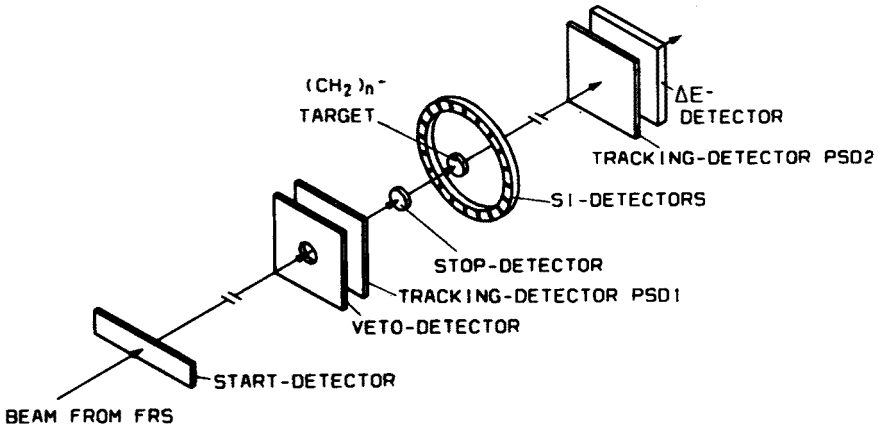

Fig. 8: Schematical view of the experimental setup for the (p,p')-experiment on ^{56}Ni (for details see text).

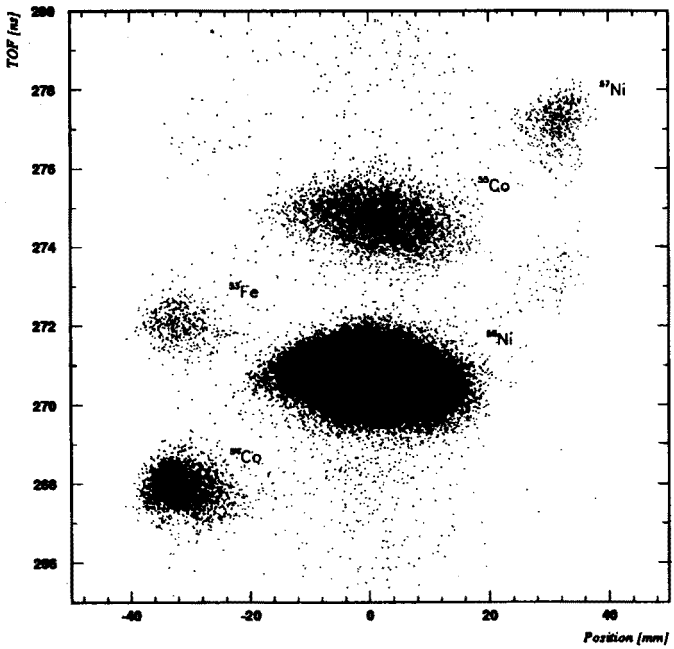

Fig. 9: Beam-properties of the ^{56}Ni-beam provided by the fragment separator. The position in x-direction, measured with a position sensitive scintillation detector (PSD1) positioned close to the $(CH_2)_n$ -target, is plotted versus the time of flight. The ^{56}Ni-beam is well centered and has a width of about 15 mm (FWHM). Impurities of neighbouring isotopes are well separated. For the isotope identification the additional ΔE-information (see fig. 8) is used.

The experimental setup is sketched in fig. 8. Total energy and time of flight of the recoil protons were measured with 18 silicon detectors (48x8 mm^2 active area each, 2500 μm thick), which had been installed inside a vacuum chamber in the geometry of a concentric ring of 20 cm radius around a 1 mg/cm^2 $(CH_2)_n$ -target. The target was mounted normal to the beam on a linear translation stage and could be moved in beam direction. Thus, an angular range of $77.5° \leq \vartheta_{lab} \leq 83.0°$ was covered. A set of scintillation detectors was used to track the beam particles and to verify their nuclear charge and mass by time of flight and energy loss measurements. As tracking detectors, two position - sensitive scintillators [35] (PSD1 and PSD2, 140x140 mm^2 active area, read out with four photomultipliers; the position information is obtained by comparing the energy signals of left/right and up/down, respectively) were mounted upstream and downstream from the target. These detectors, as well as the TOF-system, operated in vacuum and had been tested to allow for maximum beam intensities up to 10^5 sec^{-1}; a position resolution of $\Delta x \leq$ 2 mm, and a time resolution of $\Delta t \leq 250$ psec was observed. An example for the beam properties of the ^{56}Ni-beam, provided by the fragment separator for the present experiment, is displayed in fig. 9. The x-position measured with a position sensitive tracking detector (PSD1), positioned close to the target, is plotted versus the time of flight. The ^{56}Ni-beam is well centered and has a width (FWHM) of 15 mm (about the same in y-direction). Impurities of neighbouring isotopes, identified by using the additional ΔE-information (see fig. 8), are well separated. The average intensity of the ^{56}Ni-beam was about $3 \cdot 10^4$ sec^{-1}.

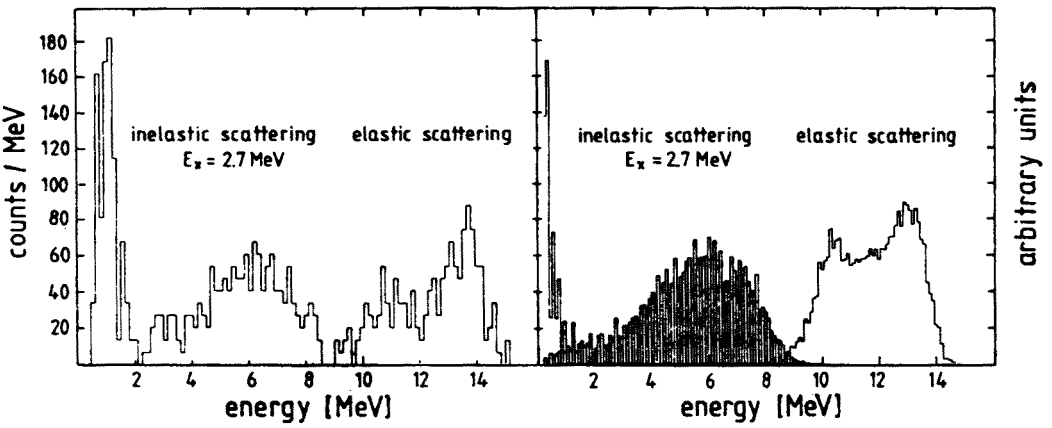

Fig. 10: Measured energy spectrum for $p(^{56}Ni,p')^{56}Ni^*$ at 100 MeV/u and $\vartheta_{lab} = 79.1°$ (left-hand side) in comparison with the expected spectrum obtained from a Monte-Carlo calculation (right-hand side). The spectra are not normalized on each other in vertical scale.

The result of a preliminary data analysis is displayed in fig. 10 (left-hand side), where the energy spectrum for the scattered protons is shown. The identification of the recoil particles was done by time of flight (time resolution ≈ 3 ns). The background originating from $^{56}Ni + {}^{12}C$-collisions was measured with pure ^{12}C-targets and subtracted from the yield obtained with the 1 mg/cm^2 $(CH_2)_n$-target. After corrections for energy loss and multiple scattering of the protons in the target, two structures appear in the energy regions, where the elastic and inelastic yields can be expected. The shape of the spectrum is in fair agreement with that resulting from a Monte-Carlo simulation (right-hand side of fig. 10), using optical model [36] and DWBA calculations, assuming $\beta_2 = 0.2$ [37]. The angular cut in inelastic scattering covers the first diffraction maximum, for elastic scattering it is near a calculated minimum in the angular distribution. Included in the simulation are multiple scattering effects of the outgoing particles in the 1 mg/cm^2 $(CH_2)_n$ -target. From the present analysis we deduce a preliminary value for the inelastic cross section in the first diffraction maximum of $(d\sigma/d\Omega) = 24.8$ mb/sr with an error at this point of the analysis of 10-20%. A more detailed analysis of the data, including the information on the scattering angle from beam tracking, is presently in progress.

IV.2. Investigation of (p,p)-Elastic Scattering on Light Neutron-rich Nuclei

This experiment aims to investigate high energy (800 MeV/u) elastic proton scattering on light neutron-rich nuclei, such as ^6He, ^8He, ^8Li, ^9Li, ^{11}Li in order to investigate their nuclear matter distribution [12] (see also section II). In the recent past extremely neutron-rich nuclei, in particular ^{11}Li, have attracted considerable attention, as a number of experimental evidences indicate that these nuclei have qualitatively new spatial structure with an extended neutron tail [14]. Various experimental results suggest the ^{11}Li-nucleus to consist of a dineutron in the field of a ^9Li-core [15]. Therefore a comparison of the nucleon distributions of ^9Li and ^{11}Li, where a different behaviour due to this giant neutron halo of ^{11}Li is expected, will be of special interest.

Due to the short nuclear lifetimes (for example $\tau = 8.7$ msec for ^{11}Li) these experiments are to be performed at an external target station without use of the ESR. The low production rates for the very neutron rich nuclei (about 10^2-10^3 sec^{-1} for ^{11}Li) demand for thick effective hydrogen targets and large solid angle detectors. To meet these experimental conditions a hydrogen-filled time - projection ionization chamber, which serves simultaneously as a gas target and a detector, will be used. The recoil detector IKAR [38] (see fig. 11), provided by the LNPI St. Petersburg, was originally developed for high energy proton-, pion-, etc., scattering [39], and is presently under reconstruction and test for the proposed experiments. It operates at a hydrogen pressure of 10 atm. The effective target length is 500 mm. The whole setup is rotationally symmetric with respect to the beam axis. It consists of six identical cells of ionization chambers, each containing a cathode, a grid and concentric anodes. The amplitude- and the drift time-analysis of the signals from the electrodes yield the proton recoil energies E_p (or ΔE_p for $E_p > 5$ MeV when the recoil protons leave the active volume), the angle θ_p of the recoil protons, and the coordinates of the interaction vertex in the grid-cathode space. The energy- and angular-resolution is $\Delta E = 120$ keV, and $\Delta\theta = 0.5°$ (for $E_p > 3$ MeV), respectively. The detector is able to stand secondary beam intensities up to the order of 10^4 sec^{-1}.

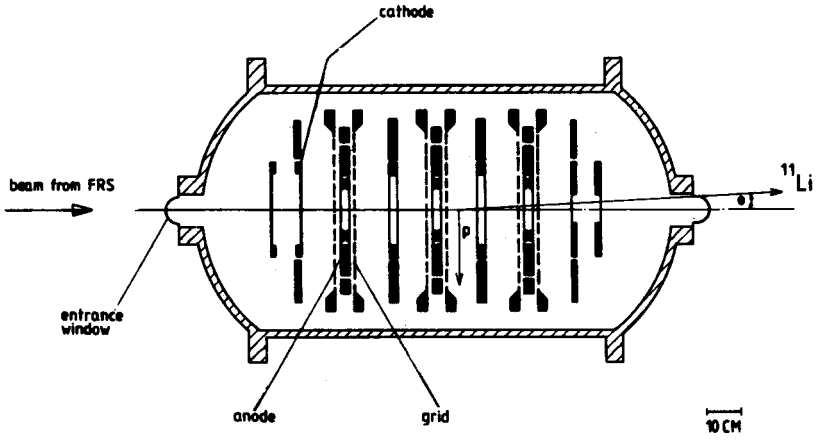

Fig. 11: Schematical view of the recoil detector IKAR used to detect scattering angle and energy of elastically scattered protons (for details see text).

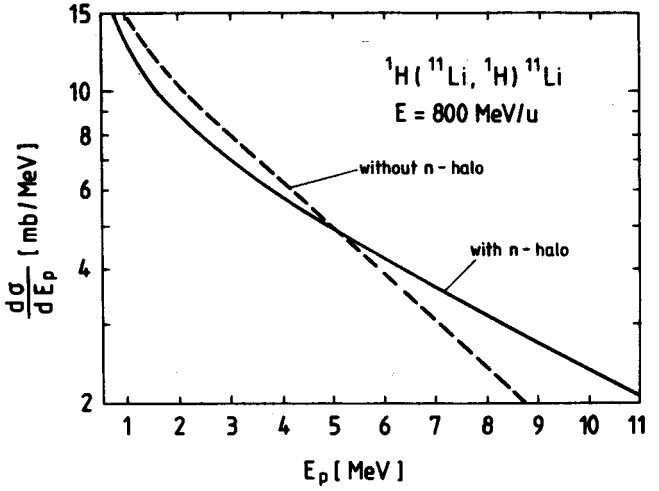

Fig. 12: Predicted differential cross sections $d\sigma/dE_p$ versus the recoil energy E_p for ^{1}H (^{11}Li,^{1}H) ^{11}Li-elastic scattering at an incident energy of E = 800 MeV/u. The calculations were performed assuming nuclear matter distributions with (solid line) and without (dashed line) a neutron-halo, but both with the same nuclear radius $< r^2 >^{1/2} = 3.6$ fm for ^{11}Li.

Figure 12 shows predictions [12,40] of differential cross sections for ^{1}H(^{11}Li,^{1}H)^{11}Li-elastic scattering at an incident energy of E = 800 MeV/u for proton recoil energies up to $E_p \leq 11$ MeV, corresponding to an angular range

$0° < \theta_{cm} \leq 6.5°$. A comparison of the solid line (calculated assuming a nuclear density distribution with a neutron halo) and the dashed line (without neutron halo) gives an idea of the sensitivity of the present experiment on the ^{11}Li neutron halo. We conclude that at these high incident energies, which allow an unambiguous analysis of the data, a good sensitivity on the neutron distribution in the region of the giant neutron halo is expected.

IV.3. Investigation of (d,p)-Transfer Reactions Using the Internal ESR Gas-Jet Target

The aim of first experiments at the internal ESR gas-target is to investigate (d,p)-reactions on nuclei in the vicinity of the doubly magic ^{56}Ni and in the A = 50-region (^{46}K, ^{56}Cr, ^{61}Fe, ^{51}Ti) of astrophysical interest. As compared to experiments at external targets we have to deal with much stronger requirements. This is because the experimental setup, including the detector systems, has to meet the UHV-conditions of the ESR.

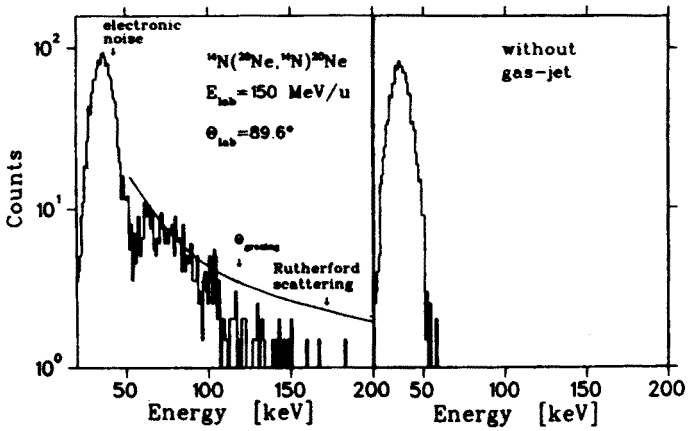

Fig. 13: Energy spectra for ^{14}N(^{20}Ne,^{14}N)^{20}Ne-elastic scattering at E_{lab} = 150 MeV/u and at θ_{lab} = 89.6° measured at the internal ESR gas target. Spectra taken with (left hand side) and without (right hand side) gas-jet are shown. The data are compared with the result of a computer simulation for Rutherford scattering (solid line).

To study the conditions of the internal gas-jet target first test measurements with stored stable beams (^{20}Ne, ^{40}Ar) have been performed using a preliminary setup which includes a relatively small solid angle detector system (Ω = 1.2 msr), mounted near θ_{lab} = 90° . This setup allows to investigate elastic scattering near the grazing angle and will be used for luminosity and beam-lifetime measurements in the ESR. A typical energy spectrum obtained for ^{14}N(^{20}Ne,^{14}Ni)^{20}Ne-elastic scattering at θ_{lab} = 89.6° is displayed in figure 13. Besides a peak due to electronic noise an energy distribution of elastically scattered ^{14}N-particles is observed, which is in good agreement with that expected for Rutherford scattering in the region below the grazing angle. The observed count rate is consistent with a luminosity of 10^{24}

cm^{-2} sec^{-1} for the present measurements and a gas-jet density of about $1x10^{10}$ atoms/cm^2. Without gas-jet only a negligible background rate is observed in the interesting region of the spectrum. The conditions of the gas-jet target have been improved recently [1]. Jet-densities at the interaction region of $6{\cdot}10^{12}$ atoms/cm^2 for Ar and $1{\cdot}10^{12}$ atoms/cm^2 for N_2 were obtained.

For the investigation of direct reactions at the internal ESR-target a new setup for the interaction region, which allows to use large solid angle detector systems in the whole angular region of interest, is presently in preparation. A schematic view of this setup is displayed in fig. 14. It consists of a beam chamber and a detector chamber. The whole setup will operate at UHV-conditions. Movable detector systems may cover the angular range $20° < \theta_{lab} < 160°$. The vertical acceptance is $\Delta\phi = \pm 20°$. The beam chamber allows to mount detectors in the angular range $0° < \theta_{lab} < -20°$ for kinematic coincidence experiments.

For the detection of the light particles we want to follow the concept of multi-detector arrays consisting of PIN-diodes, which provide excellent energy resolution ($\Delta E \leq 30$ keV for 5.5 MeV α-particles [42], and are available at relatively low cost, thus allowing to cover large solid angles. Fig. 15 displays the layout of a prototype detector consisting of 100 PIN-diodes (1 cm^2 active area each) in a 10x10 quadratic arrangement. In order to reduce the amount of electronics a semicollective readout method was used, which allows to obtain energy and time signals from each of the 100 PIN-diodes with only 20 electronic channels. For that purpose the 10 PIN-diodes in each row are connected at their N - contacts and the 10 PIN-diodes in each column at their P - contacts. The 10 rows deliver the energy signals, the 10 columns the time signals, and by a coincidence - condition the identification of the diode which fires is obtained. This scheme only works reliably, if multiple-hit events are rare, which is the case for our studies. The prototype detector was used in a test experiment [42] with a stable ^{136}Xe-beam from the UNILAC-accelerator, where the d(^{136}Xe,p)^{137}Xe*-reaction leading to excited states of ^{137}Xe was investigated at E = 5.9 MeV/u using the method of inverse kinematics. For that purpose a deuterated Ti-foil (100μg/cm^2, Ti:D-content 1:1) was used as a target. A typical energy spectrum obtained at $\theta_{lab} = 120.8°$ is displayed in fig. 16. Peaks corresponding to transitions to the strong single-particle states in ^{137}Xe are clearly resolved on a continuous background. A detailed energy versus time-of-flight analysis showed, that the dominant part of this background (≥90%) consists of protons, most likely evaporation protons from the Xe + Ti reaction. The observed energy resolution was of the order of $\Delta E = 80$ keV, mainly determined by the angular resolution. It may be improved by enlarging the distance target-detector and by using better quality beams, e.g. cooled beams of the ESR. For first measurements of (d,p)-reactions at the ESR PIN-diode detector arrays consisting of 16x16 PIN-diodes, well suited for the UHV-conditions of the ESR (bakable up to temperatures of 200°C), are presently in preparation.

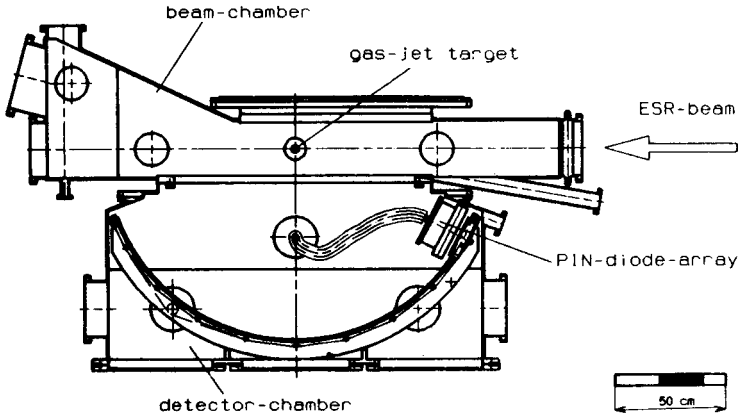

Fig. 14: Schematic view of the future experimental setup at the internal gas target. It consists of a beam chamber housing the interaction region between the stored beam and the gas-jet target, and a detector chamber. The detector chamber will contain arrays of PIN-diodes which are movable in the angular range $20^{\circ} < \theta_{lab} < 160^{\circ}$.

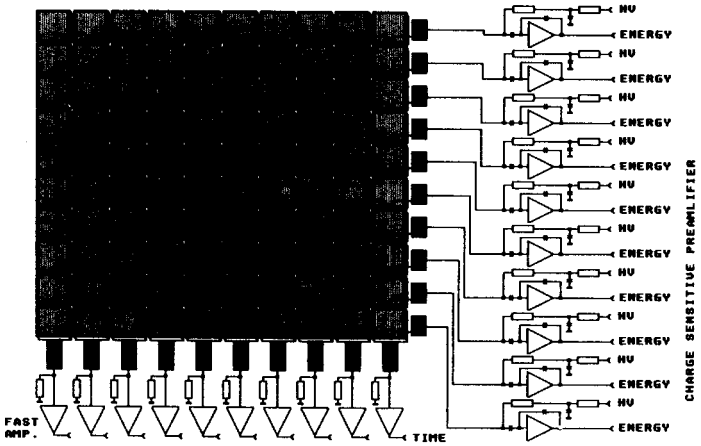

Fig. 15: Schematic diagram of a PIN-diode array in a 10x10 quadratic arrangement and the electronic matrix readout.

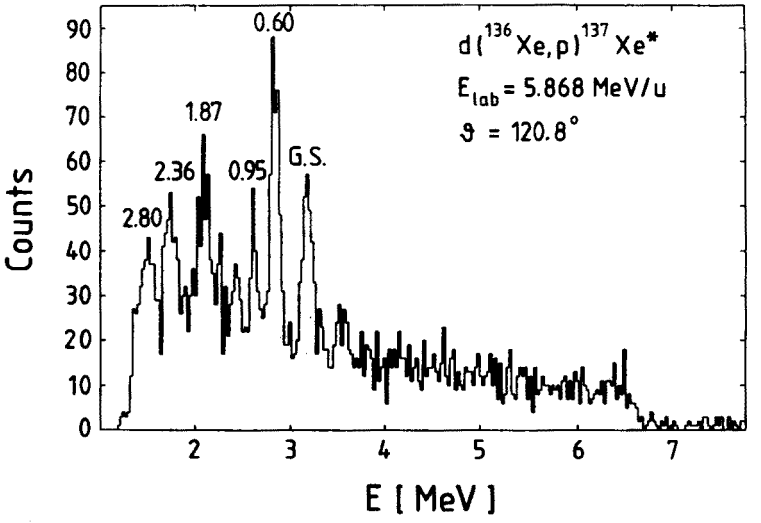

Fig. 16: Energy spectrum of protons emitted in the reaction $d(^{136}Xe,p)^{137}Xe^*$ at $\vartheta_{lab} = 120.8°$.

V. Conclusions

The combination of the new heavy-ion facilities SIS, FRS and ESR at GSI opens new possibilities for a large variety of nuclear studies. The method of inverse kinematics with good quality exotic beams allows for nuclear structure studies on nuclei in the region away from stability by investigating light ion induced reactions, such as transfer reactions, inelastic and elastic scattering. The physics motivation for such investigations was discussed in detail. Some of the most interesting questions focus on

- the test of the nuclear shell model in the region away from stability,
- the investigation of matrix elements of the 2-body residual interaction,
- astrophysical aspects, such as the understanding of the synthesis of stable isotopes in stellar burning processes,
- the investigation of nuclear matter distributions of (light) neutron rich nuclei,
- information on collective strength and transition densities, etc..

The conditions for exotic beams at GSI, namely the high energies available and the high quality cooled beams from the ESR, allow addressing at least some of these questions. Nevertheless, it should be kept in mind that we are dealing with "secondary reaction experiments" where cross sections of the order of a few millibarns limit the event rates twice, first in producing the exotic beams, secondly when investigating the reaction of interest. This leads to the following essential requirements for most of the experiments:

- highest luminosities available for both steps mentioned above,

- large solid angle detector systems, for example arrays of PIN-diodes, or active gas targets such as time-projection ionization chambers,
- external and internal ESR-targets, dependent on the specific conditions (nuclear lifetimes, level spacings, etc.),
- high resolution and high luminosities provided by the ESR through cooling and stacking.

First generation experiments, which are presently in preparation or recently performed, are (p,p′) and (p,p)-scattering on ^{56}Ni and light neutron-rich nuclei such as ^{6,8}He, and ^{8,9,11}Li, as well as (d,p)-reactions on A≈50-nuclei. The investigation of one of the regions of most interest near the doubly magic ^{132}Sn will need considerable improvements of the experimental conditions for a successful realization.

Acknowledgements

The author is indepted to B. Franzke, H. Geissel, W. Henning, G. Münzenberg and J.P. Schiffer for many stimulating discussions. The experimental work reported was performed in collaboration with: L.V. Chulkov, C. Fischer, B. Franzke, J. Friese, H. Geissel, A. Gillitzer, M. Golovkov, A. Gruber, M. Hamm, W. Henning, A. Himmler, H.J. Körner, J.V. Kratz, G. Kraus, R. Kulessa, A. Magel, G. Münzenberg, F. Nickel, A. Ogloblin, M. Peter, J.P. Schiffer, W. Schwab, D. Vieira, W. Walus, A. Weiss.

References

1. B.Franzke, K. Beckert, F. Bosch, H. Eickhoff, A. Gruber, O. Klepper, F. Nolden, U. Schaaf, P. Spädtke, M. Steck,
and K. Blasche, B. Franczak, Contributions to the 3rd European Particle Accelerator Conference, Berlin (1992), GSI-Preprint GSI-92-25
2. H. Geissel et al., Nucl. Instr. Meth. B70 (1992) 286
3. G. Mairle, Z. Phys. A322 (1985) 173
and M. Seeger, Th. Kihm, K.T. Knöpfle, G. Mairle, U. Schmidt-Rohr, J. Hebenstreit, D. Paul, P. von Rossen, Nucl. Phys. A533 (1991) 1
4. P. Egelhof, H. Emling, G. Graw, E. Grosse, W. Henning, H.-J. Körner, J.V. Kratz, K.L. Kratz, R. Kulessa, G. Rosner, J.P. Schiffer, W. Wagner, H.J. Wollersheim, Nuclear Structure Studies Near Closed-Shell-Nuclei far off Stability, proposal no. S56 for the SIS/ESR experimental programm, GSI Darmstadt, Germany (1988), unpublished
5. W.W. Daehnick, Phys. Rep. 96 (1983) 317
6. J.J. Cowan, F.-K. Thielemann, J.W. Truren; Phys. Rep. 208 (1991)269
7. T. Lee et al., Astrophys. J. 220 (1978) L21, and 228 (1979) L93
D. Bodansky et al., Astrophys. J. Suppl. Ser. 148 (1968) 16
J.L. Birck, G.W. Lugmair, Earth and Planetary Science Letters 90 (1988) 131
J. Völkening, D.A. Papanastassiou, Astrophys. J. Letters (1989) L43
8. K.L. Kratz et al., Proc. First Europ. Biennial Workshop on Nucl. Phys., Megève, France 1991, World Scientific ISBN 981-02-0839-1 (1991) 218, and references therein
9. D. Hartmann, S.E. Woosley, M.F. El Eid, Astrophys. J. 297 (1985) 837,
and F.-K. Thielemann, K.-L. Kratz, B. Pfeiffer, P. Möller, W. Hillebrandt, Proc. of the Int. Symp. on Nucl. Astrophys. Baden/Vienna, Austria, 1990, H. Oberhummer, W. Hillebrandt (eds.) (1990), p. 286
10. K.L. Kratz, private communication
11. A.E. Champagne, M. Wiescher, Ann. Rev. Nucl. and Part. Sci., to be published
12. G.D. Alkhazov, N.M. Andronenko, N.F. Bondar, A.V. Khanzadeev, G.A. Korolev, A.A. Lobodenko, V.A. Mylnikov, G.E. Petrov, D.M. Seliverstov, E.M. Spiridenkov, A.A. Vorobyov, P. Egelhof, H. Geissel, W. Henning, A. Magel, G. Münzenberg, M. Mutterer, U. Nast-Linke, J. Theobald, Study of Nucleon Density Distributions in Light Neutron-Rich Radioactive Nuclei by Proton Elastic Scattering in Inverse Kinematics, proposal no. S105 for the SIS/ESR experimental program, GSI Darmstadt, Germany (1991), unpublished
13. G.D. Alkhazov, S.L. Belostotsky, A.A. Vorobyov, Phys. Reports 42C (1978)89
14. I. Tanihata, Nucl. Phys. A522 (1991) 275
15. L. Johannsen, A.S. Jensen, P.G. Hansen, Phys. Lett. B244 (1990) 357
16. C.-B. Moon, M. Fujimaki, N. Inabe, K. Katori, J.C. Kim, T. Kobayashi, T. Kubo, H. Kumagai, S. Shimoura, T. Suzuki, I. Tanihata, Proc. of the 6th Int. Conf. on Nuclei far from Stability, 1992, Bernkastel-Kues, Germany, to be published
17. A. Ogloblin, L.V. Chulkov, A.S. Demyonova, V.I. Dukhanov, P. Egelhof, W. Henning, M.S. Golovkov, E.F. Svinazeva, Elastic Scattering of ^{14}C- and ^{14}O-ions on ^{16}O- and ^{18}O-targets, proposal no. E011 for the SIS/ESR experimental program, GSI Darmstadt, Germany (1990), unpublished
18. P. Schwandt, Proc. of the Int. Nuclear Physics Conference Sao Paulo, Brasil 1989 (M.S. Hussein, E.F. Pessoa, A.F.R. de Toledo Piza, O. Sala, A. Szanto de Toledo, L.F. Canto, R. Donangelo, eds.), World Scientific, Vol. 2 (1990) 133

19. H. Geissel et al., Proceedings of the Int. School Seminar on Heavy ion Physics, Dubna, USSR, 1989
20. A. Gruber, W. Bourgeois, B. Franzke, A. Kritzer, C. Treffert, Nucl. Instr. Meth. A282 (1989) 87
21. F. Bosch, Nucl. Instr. Meth. A314 (1992) 269
22. H. Geissel, K. Beckert, F. Bosch. H. Eickhoff, B. Franczak, B. Franzke, M. Jung, O. Klepper, R. Moshammer, G. Münzenberg, F. Nickel, F. Nolden, U. Schaaf, C. Scheidenberger, P. Spädtke, M. Steck, K. Sümmerer, A. Magel, Phys. Rev. Lett. 68 (1992) 3412
23. G.R. Satchler, Direct Nuclear Reactions, Clarendon Press, Oxford, Oxford University Press (1983)
24. C. Ekström, Proc. LAS, Uppsala, Sweden, CERN Report 90-04 (1990) 184
25. D. Fick, E. Steffens, private communication
26. K. Sümmerer et al., Phys. Rev. C42 (1990) 2546
27. G. Kraus et al., Proc. of the 6th Int. Conf. on Nuclei far from Stability, 1992, Bernkastel-Kues, Germany, to be published, and G. Kraus et al. to be published
28. L.W. Woo, N.S. Wall, P.G. Roos, P.H. Debenham, K. Kwiatowski, A. Nadasen, Phys. Rev. C29 (1984) 794
29. G. Münzenberg, Proc. of the Int. Workshop on the Physics and Techniques of Secondary Beams, Dourdan, France, 1992, to be published
30. A.S. Schlachter, J.W. Stearns, W.G. Graham, K.H. Berkner, R.V. Pyle, J.A. Tanis, Phys. Rev. A27 (1983) 3372
31. Th. Stöhlker, C. Kozhuharov, A. E. Livingston, P.H. Mokler, Z. Stachura, A. Warczak, Z. Phys. D23 (1992) 121
32. Th. Stöhlker, private communication
33. N. Schulz, J. Chevallier, B. Haas, J. Richert, M. Toulemonde, Phys. Rev. C8 (1973) 1779
34. S. Raman, C.H. Malarkey, W.T. Milner, C.W. Nestor, Jr., P.H. Stelson, Atomic Data Nucl. Data Tables 36 (1987) 1
35. H. Spiess, PhD-thesis, Frankfurt (1992), GSI Report 92-12
36. K. Kwiatowski et al., Nucl. Phys. A301 (1978) 349
37. L.W. Woo et al., Phys. Rev. C29 (1984) 794
38. A.A. Vorobyov, G.A. Korolev, V.A. Schegelsky, G.Y. Solyakin, G.L. Sokolov, Y.K. Zalite, Nucl. Instr. Meth. 119 (1974) 509
39. J.P. Burq et al., Nucl. Phys. B187 (1981) 205,
J.P. Burq et al., Nucl. Phys. B217 (1983) 285,
O.G. Grebenjuk et al., Nucl. Phys. A500 (1989) 637
40. G.D. Alkhazov, A.A. Lobodenko, Proc. of the 6th Int. Conf. on Nuclei far from Stability, 1992, Bernkastel-Kues, Germany, to be published
41. J. Friese, H.J. Körner, C. Schießl, W. Wagner, G. Kraus, GSI Scientific Report 1989 (U. Grundinger ed.), GSI Darmstadt (1990) 297
42. G. Kraus, P. Egelhof, H. Emling, E. Grosse, W. Henning, R. Holzmann, H.J. Körner, J.V. Kratz, R. Kulessa, Ch. Schießl, J.P. Schiffer, W. Wagner, W. Walus, H.J. Wollersheim, Z. Phys. A340 (1991) 339